
D4.2 INTERIM ENVIRONMENTAL REPORT

Horizon 2020 – ELEMENT

Document Number: ELEMENT-EU-0011



DOCUMENT HISTORY

FIELD	DETAIL
REPORT TITLE	Interim environmental report
REPORT SUB-TITLE	Interim environmental report on site resource characterisation and environmental impact model, to inform test system design
CLIENT/FUNDING	H2020
STATUS	Final Version
PROJECT REFERENCE	ELEMENT
DOCUMENT REFERENCE	ELEMENT-EU-0011

REVISION	DATE	PREPARED BY	CHECKED BY	APPROVED BY	REVISION HISTORY
V0	29/05/2020	FEM	NOVA		Original Draft
V1	30/06/2020	FEM	NOVA	NOVA	Submitted version



TABLE OF CONTENTS

Executive summary	3
Acknowledgment	4
Abbreviations and acronyms	5
Context and objectives	6
Selection of test location at Etel river	7
Etel site resource characterisation	9
Data analysis and methods.....	9
Results.....	10
Conclusions and next steps	13
Bluemull Sound characterization	14
Data analysis and methods.....	14
Results.....	15
Environmental impact monitoring: pre-design work	18
Perspectives	20
References	21



Executive summary

A Funding Grant was awarded from the European Union's Horizon 2020 research and innovation programme to develop and validate an innovative tidal turbine control system, using the tidal turbine itself as a sensor, to deliver a step change improvement in the performance. This will demonstrate Effective Lifetime Extension in the Marine Environment for Tidal Energy (ELEMENT), driving the EU tidal energy sector to commercial reality. This report focuses on the characterization of the hydrokinetic resource and turbulence at the future tidal turbine testing sites, in Etel River as well as Bluemull Sound. This report summarizes the analysis of existing hydrokinetic data from both sites. In addition, the monitoring options that can enhance the design work under the ACAS (Automated Collision Avoidance System) are discussed.

At Etel Site, a 12.5 day-period, containing a full spring tide tidal cycle, was analyzed. Results on cumulative occurrence of the velocity magnitude suggest that a tidal turbine with a cut-in-speed of 0.5 m/s might generate electricity, 80% of the time. Moreover, the flow at Etel site is ebb-dominated. A substantial asymmetry in velocity magnitude recorded during flood and ebb tide was found. This asymmetry generates considerable gap in kinetic power density during both tidal phases with kinetic power density more than 3 times higher during ebb tide than flood tide. The turbulence intensity and the integral lengthscale were quantified along the three spatial directions. For both metrics, the streamwise direction is associated with the highest values. The depth-averaged streamwise turbulence intensity and the integral lengthscale was found to be 5% and 7.5 m.

At Bluemull site (Shetland), three 5-beam ADCPs were deployed in three locations North of the three operational M100 turbines at depths of approximately 30-35m. Cumulated occurrences of flow velocity magnitude indicate that 0.5 m/s and 1 m/s are exceeded 90% and 70% of the time respectively. The flow magnitude between flood and ebb tide was found to be globally symmetric. For flow velocity higher than 1 m/s, the turbulence intensity was found to be ranging from 12 to 20%.

The monitoring options that can enhance the design work under the Automated Collision Avoidance System (ACAS) have been the subject of discussions between FEM and Nova. The aim of discussions was to review the benefits of different methods of monitoring near-field interactions between marine life (more particularly mammals, birds and fish) and turbines. Exchanges between FEM and Nova have strengthened the general idea of developing a monitoring strategy combining sonar and digital cameras in order to gain in situ data that will enhance predictions of encounter and collision risk.



Acknowledgment

The ELEMENT project would like to thank GUINARD ENERGIES and IFREMER for their support. The data analysis performed at Etel test site relies on data acquired within the MEGAWATTBLUE project performed by GUINARD ENERGIES and IFREMER.

The ELEMENT project would like to thank the members of the EnFAIT project. The ELEMENT project benefits from the existing data and infrastructure developed during the EnFAIT project, and this report relies on data and analysis of the Bluemull Site carried out within the EnFAIT project.



Abbreviations and acronyms

ACAS: Automated Collision Avoidance System
ADCP: Acoustic Doppler Current Profiler
ADV: Acoustic Doppler Velocimeter
CRM: Collision Risk Model
ESA: Environmental and Social Acceptance
EnFAIT: Enabling Future Arrays in Tidal
MRE: Marine Renewable Energy
STA: Shetland Tidal Array



Selection of test location at Etel river

One purpose of WP4 is to identify the optimum test location at Etel river, considering the velocity fields and consenting issues. This task has been performed already in the framework of the MegaWattBlue project, led by Guinard Energies. This task was completed by Ifremer. Considering that both theoretical yield and consenting issues are relatively device agnostic, it was decided that using the findings of this existing analysis presented best value to the project.

An evaluation framework was developed to identify locations with a potential for energy harvesting. In order to select the optimum location of the Guinard Energies' tidal turbine P154, two conditions were considered to select the optimum test location:

- Hydraulic energy yield, i.e., the theoretical energy yield available in the tidal current;
- Administrative, legal and practical aspects, including nautical constraints.

Hydraulic energy yield was evaluated through the use of a 2D hydrodynamic model. The outputs of this model are confidential and cannot be presented in this report. Following both conditions, an area corresponding to a rectangle of 100 m x 20 m was selected to undertake tidal turbine testing (Fig. 2).

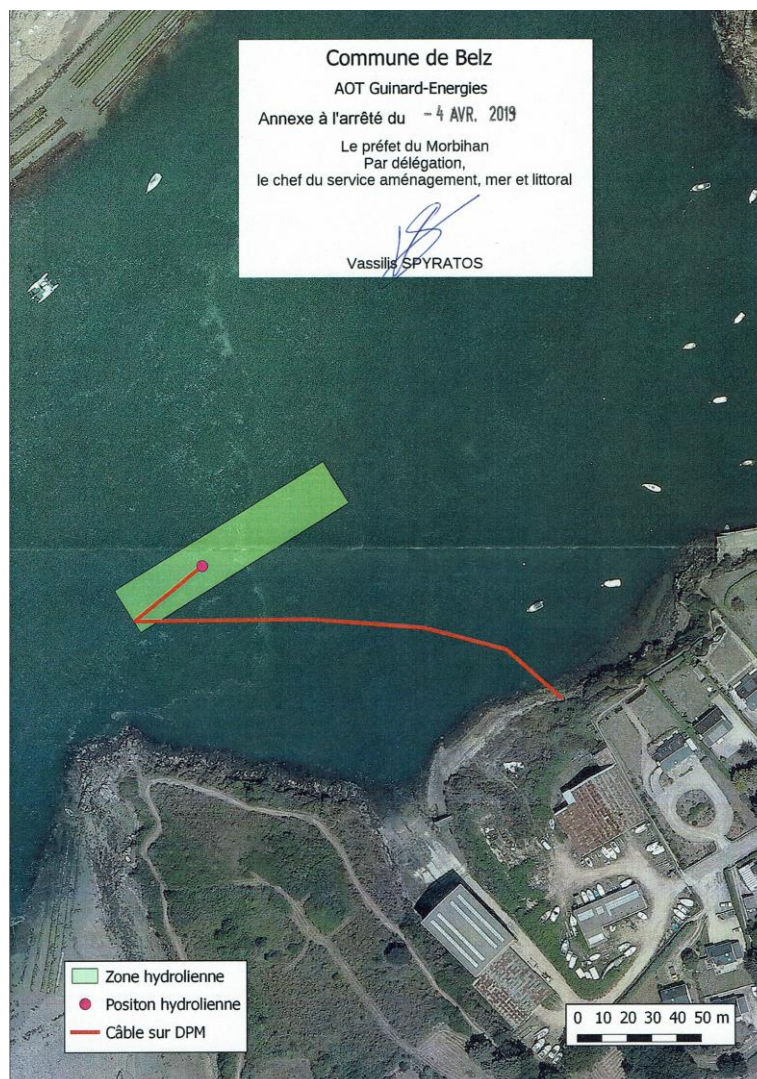


Fig. 2 – Aerial photograph of the Etel river with the location of the area consented to undertake tidal turbine testing (green rectangle), position of the tidal turbine P154 of Guinard Energies and electrical cable.

In 2012, Guinard Energies started the process of applying for a consent at Etel river. A first authorisation for tidal turbine testing, including a floating platform in the consented area was delivered on the 5th June 2015 for a duration

of three years, and a prolongation was authorized on 1st November 2018 for a duration of three further years. The authorization covers the installation, the realisation of technical tests and dismantling of a system constituted by a tidal turbine, its cable and a technical building.

Following consideration of device specific factors (e.g water depth and target flow speeds), the location selected for testing of Guinard Energies P154 turbine has been assessed as also being suitable for the tidal turbine of Nova Innovation.

In order to ease the consenting process in the frame of ELEMENT, and as the authorized area is located at the optimum place in regards to (i), hydraulic energy yields and (ii), administrative, legal and practical aspects, the partners decided that the preferred course of action was to perform the tests of Nova Innovation tidal turbine in Etel river within the area consented to Guinard Energies. To that purpose, discussions are ongoing with all key stakeholders to ensure all required agreements and permits are in place prior to the test phase.



Etel site resource characterisation

Data analysis and methods

Experimental settings

In the frame of the MegaWattBlue project, a Nortek Sentinel 1 000 kHz five-beam ADCP was deployed on the seafloor (mean and maximum water depth of 15.5 m and 17.5 m respectively) approximately 100 m off the site of Chantier Bretagne Sud, in the Etel River. The ADCP collected data over a 33-day period, from 7 June to 10 July, 2018. The ADCP was set to record continuously the velocities in beam and instrument coordinates at the pinging rate of 8 Hz. Velocities were recorded with 0.5 m vertical resolution (bin size), starting 1.2 m from the seafloor (centre of the first bin).

A period of approximately 12.5 days, i.e., from 7 to 19 June 2018, with a full spring tide cycle was selected for the analysis. This period exhibited the highest tidal current velocity magnitudes. The selected period was divided into 1794 subsets of 10-min each. The 10-minutes duration is of sufficient length to provide a good sample of the largest turbulent eddies, but not so long that the turbulent processes cannot be regarded as quasi stationary.

The present study focuses on turbulence characterization along the streamwise, spanwise and vertical direction of the current associated respectively with the vectors \vec{e}_x , \vec{e}_y and \vec{e}_z (Fig. 3). Horizontal velocity components recorded by the ADCP in instrument coordinates were projected on along- and cross-stream axes of the river. The projection angle (34° clockwise) matches the orientation of the tidal current ellipse throughout the water column.

The average standard deviation of the pitch and roll of the ADCP were found to be lower than 0.5°, and that of the heading lower than 2°. These low values indicate that the frame remained stable throughout the deployment.

The following metrics were quantified: (i) - the velocity, (ii) - the turbulence intensity, (iii) - the integral lengthscale, and (iv) - five components (out of six) of the Reynolds stresses. The methodology used to characterize these metrics is described in the first deliverable (D4.1) of the work package 4 of the ELEMENT project. All metrics are evaluated in three-dimension (3D), i.e., along the streamwise, spanwise and vertical velocity. There is broad agreement that these turbulence metrics contribute significantly to turbulence-induced hydrodynamics loads on tidal turbines. The aim of this study is to characterize the tidal dynamics at Etel site and provide modelers and tidal turbine designers with mean profiles of the turbulence metrics throughout the water column allowing them to build a dedicated methodology for fatigue life prediction of moving component.

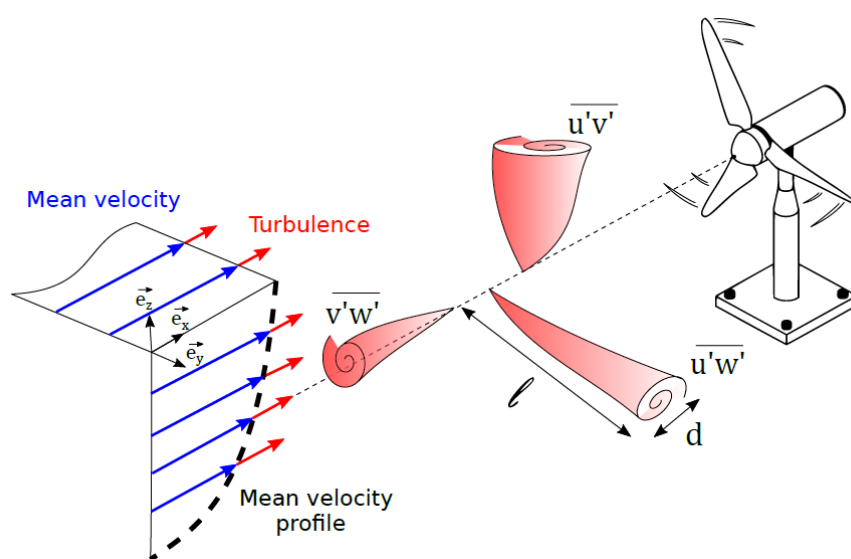


Fig. 3 - Schematic of turbulent inflow to a tidal-stream energy converter. The mean-flow profile is represented in blue, and turbulent eddies of different characteristic sizes (d), lengths (l), and orientations are indicated in red.

Results

Tidal dynamics and energy resource characterization

Fig. 4 shows time series of the Sea Surface Height (SSH) and the depth-averaged streamwise velocity. SSH evolves from 14 m to 17.5 m with a mean of 15.5 m. Tidal variations of SSH and currents are predominantly semi-diurnal and globally symmetric. Peak flood and ebb tidal velocities occur at high and low water respectively with slack water at mid-tide. The tidal current dynamics is thus referred to as progressive wave system.

Velocity histograms provide a simple way to evaluate the available resource at any point of a site. They indicate what percentage of time could be used for power generation. Fig. 5 shows the cumulated occurrence of the depth-averaged velocity magnitude. The cut-in-speed of a typical tidal turbine ranges between the velocity value of 0.5 m/s and 1 m/s. The histograms of velocity magnitude show that both velocity values of 0.5 m/s and 1 m/s are exceeded respectively 80% and 40% of time at Etel site.

Fig. 6a exhibits a clear imbalance of the velocity magnitude. The current asymmetry, i.e., the ratio of the mean velocity during flood tide to the mean velocity during ebb tide was found to be 0.7 on average revealing that the tidal flow is ebb dominated. Since the kinetic power density P as well as the output power generated by a tidal turbine is related to the velocity cube, a high current asymmetry can generate significant difference in power production between the flood and ebb phase of the tide. Considerable difference in kinetic power density between both flood and ebb tide is exhibited in Fig. 6b. During flood and ebb tide, the depth-averaged value of P reaches 1.2 kW/m² and 4.2 kW/m² respectively. The mean kinetic power density during flood tide was found to be 0.4 kW/m² whereas that estimated during ebb tide is more than 3 times higher, i.e., 1.25 kW/m². This result reveals that, during ebb tide, the mean value of P is higher than the maximum value reaches during flood tide.

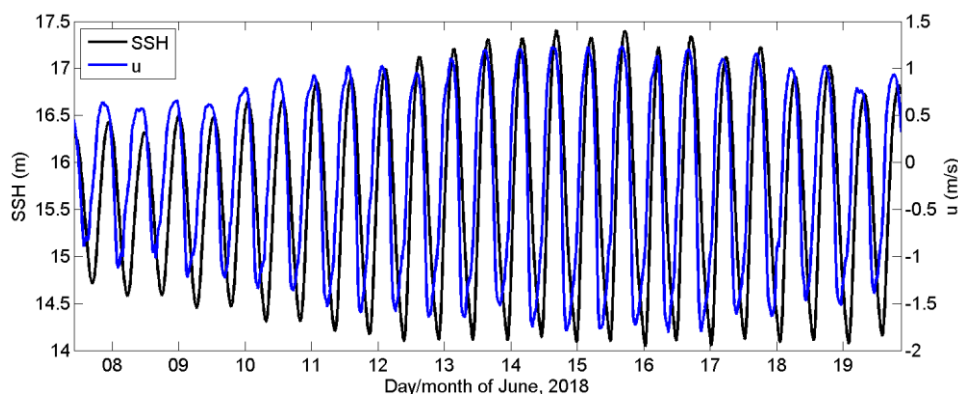


Fig. 4 – Time series of the sea surface height (SSH) and the depth-averaged streamwise velocity (u).

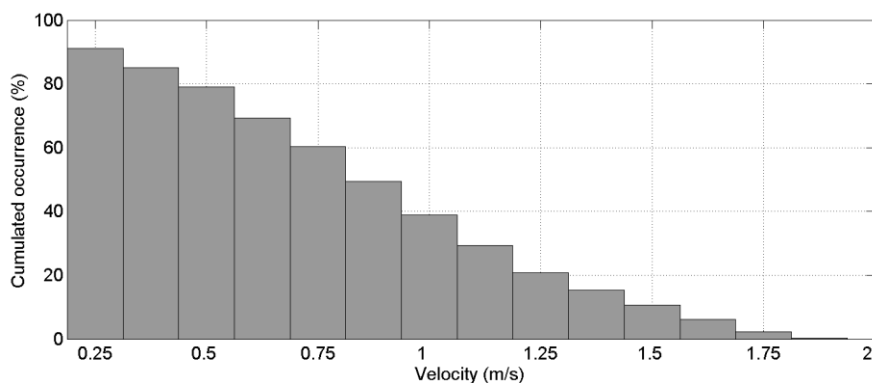


Fig. 5 – Cumulative occurrence of the depth-averaged velocity magnitude.

Mean vertical profiles of the absolute value of the streamwise (u), spanwise (v) and vertical (w) velocity were computed (Fig. 7a). The profiles were averaged over the 12.5 day-period. The profiles associated with the streamwise



velocity show an uncommon behavior: the velocity increases with increasing height above bottom until a height of 6 meter above bottom (m.a.b), remains constant between 6 and 8 m.a.b and decreases above. This decreasing is not common. A sudden variation of bathymetry in the vicinity of the ADCP location with a sharp negative slop might explain such behavior. The spanwise and vertical velocity remains nearly-constant throughout the water column with value slightly evolving from 0.15 m/s and 0.05 m/s respectively. The depth-averaged value of the streamwise velocity (absolute value) was found to be 0.85 m/s with peak velocity of 1.9 m/s during ebb tide and 1.3 m/s during flood tide.

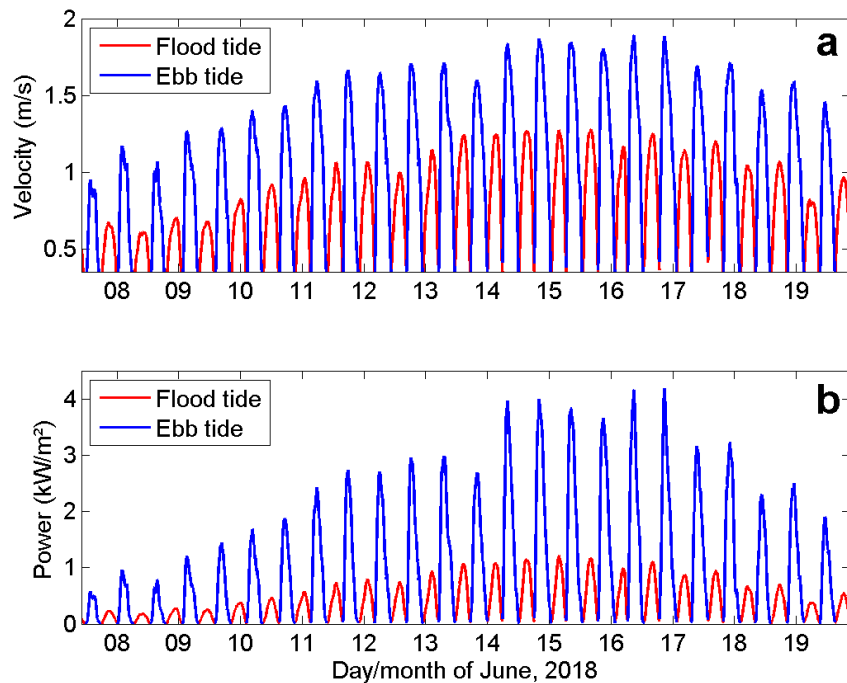


Fig. 6 – Time series of the depth-averaged velocity magnitude (a) and kinetic power density P (b). Red and blue colors are used to identify flood and ebb tide respectively.

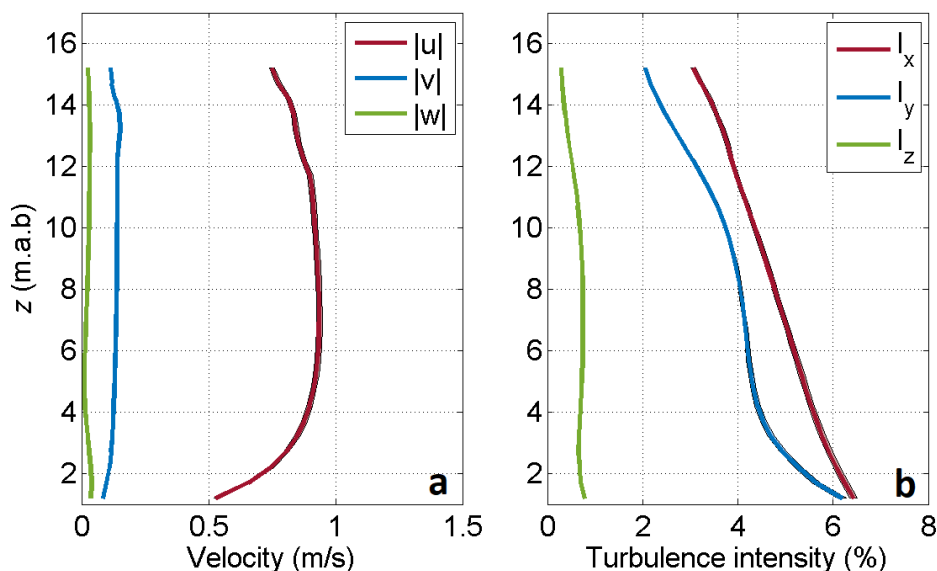


Fig. 7 – Mean vertical profiles of the velocity (a) and the turbulence intensity (b) estimated along the streamwise (red), spanwise (blue) and vertical (green) direction. The profiles were averaged over the 12.5 day-period.

Turbulence

Turbulence intensity

The turbulence intensities were corrected from Doppler noise resulting in a considerable reduction of the streamwise (I_x), spanwise (I_y), and vertical (I_z) turbulence intensity by 40%, 35% and 30% respectively. The Doppler noise was found to be increasing with increasing flow speed and to be independent of the height above bottom (results not shown). Such high contamination is the result of the low bin size (0.5 m here). It is well known that low bin size generates a high Doppler noise whereas high bin size is associated with low Doppler noise (Guerra and Thomson, 2017; Thiébaud et al., 2019). Setting the bin size at a higher value (ex, 1 m) would have considerably reduced the Doppler noise. However, this would have induced a loss in vertical resolution of velocity measurements and, thus, a loss in the variety of turbulence structure sizes that can be captured by the ADCP. There is trade-off to make.

To date, several studies focusing on the characterization of the turbulence intensity have been performed within tidal channels. Most of the studies focused on the streamwise turbulence intensity, (I_x), which is generally considered as the turbulence metric most relevant to the unsteady loading on TECs. Fig. 8b shows time series of the depth-averaged streamwise turbulence intensity. (I_x) was found to be varying in a wide range: from 0.5% to 14.5% with a mean value of 5%. It can be seen that (I_x) is systematically lower during periods when the water level is lower than the mean water level and is higher when the water level is higher. There seems to be a quadrature between (I_x) and SSH, and therefore between (I_x) and (u). At mid-tide, (I_x) change abruptly from the highest values to the lowest one. Similar behavior was identified for both (I_y) and (I_z) (results not shown).

Fig. 7b shows the variation of the turbulence intensity (I_i) throughout the water column. The three components of the turbulence intensity decrease with increasing height above bottom. The streamwise turbulence intensity is constantly higher than that associated with the spanwise and vertical direction. On average, the ratios I_x/I_y and I_x/I_z were found to be 1.2 and 7.5 respectively.

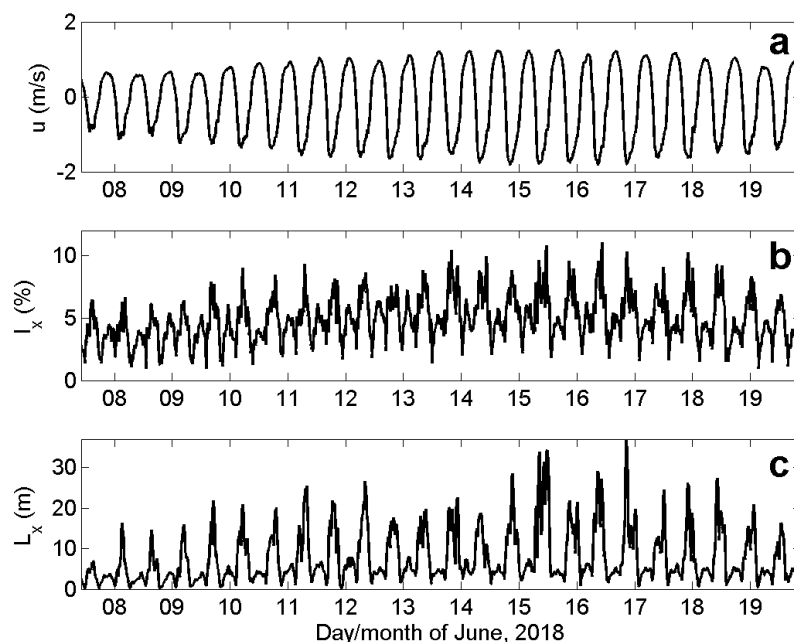


Fig. 8 – Time series of the depth-averaged velocity u (a), turbulence intensity I_x (b) and integral lengthscale L_x (c) associated with the streamwise direction.

Integral lengthscale

The integral lengthscales were quantified. The dynamics of the large-scale turbulent eddies (i.e., the integral lengthscale) was found to be clearly anisotropic with predominantly horizontal motions at scales greater than the local water depth. These eddies contain the largest proportion of turbulent energy, and are therefore likely to have the greatest effect on TECs performance. Fig. 8c shows the time series of the depth-averaged integral lengthscale, (L_x), associated with the streamwise direction. (L_x) was found to be ranging between 0.5 m and 35 m with a mean



of 7.5 m. (L_x) is clearly modulated by (u). The integral lengthscale is dependent on the flow speed and increases with increasing flow speed. Maximum integral lengthscales are associated with both peak flood and ebb velocity with values of (L_x) slightly higher during flood tide. Throughout the water column, (L_x) was found to be constantly higher than the integral lengthscale associated with spanwise and vertical direction, i.e., (L_y) and (L_z) respectively with depth-averaged ratio L_x/L_y and L_x/L_z of 1.3 and 3.6 respectively.

Conclusions and next steps

This report focuses on the characterization of the hydrokinetic resource and turbulence at the future tidal turbine testing site, in Etel River. The area most relevant for such testing was previously identified in the framework of the MegaWattBlue project. The dimensions of this area are small enough (100 m x 20 m) to consider that the hydrodynamics study presented in this report is indicative for the full area. Results are based on 5-beam ADCP measurements. A period of 12.5 days, containing a full spring tide tidal cycle, was selected for the analysis.

Results on cumulative occurrence of the velocity magnitude suggest that a tidal turbine with a cut-in-speed of 0.5 m/s might generate electricity, 80% of the time. Moreover, a substantial asymmetry in velocity magnitude recorded during flood and ebb tide was found. The flow at Etel site is ebb-dominated. This asymmetry generates considerable gap in kinetic power density during both tidal phases with kinetic power density more than 3 times higher during ebb tide than flood tide.

A turbulence analysis was carried out. The values of the turbulence intensity were considerably affected by Doppler noise. The former was quantified in order to properly quantify the turbulence intensity. However, other measurements are required to confirm our results. Such high Doppler noise was induced by the small bin size which was set to 0.5 m. In order to reduce the Doppler noise, it is recommended to increase the bin size. Setting the bin size to 1 m seems to be a good trade-off between the reduction of Doppler noise and the size of the turbulent structures that can be captured by an ADCP. This setting will be applied for the upcoming ADCP deployments.

Mean profiles of the turbulence intensity were evaluated. The streamwise turbulence intensity (I_x) is the primary load driver for horizontal axis-TECs (Milne et al., 2010). (I_x) was found to be systematically higher than the spanwise (I_y) and vertical (I_z) turbulence intensity.

The size of the most energetic turbulent eddies was quantified along the three spatial directions. However, the depth averaged value of the integral lengthscale associated with the streamwise direction was found to be 7.5 m. This value is higher than the diameter of the Nova Innovation tidal turbine that will be used during testing. Recently, a study focusing on the assessment of the performance of a Darrieus type turbine operating in real sea conditions demonstrated that the strongest impact of turbulence on power generation by the TEC occurred when the length of the most energetic eddies matches the turbine size (Sentchev et al., 2019). The authors show that these eddies exert periodic loads on the blades, strongly affect torque and cause power pulsations.

However, although the integral lengthscale is a dominant driver of the fatigue loads exerted on TECs blades, it is not the primary load driver for horizontal-axis TECs. A parametric assessment of the sensitivity of the fatigue loads of TEC blades indicated that the integral lengthscales have a much smaller role than the turbulence intensity (Milne et al., 2010).



Bluemull Sound characterization

Data analysis and methods

All data and models used in the characterization of Bluemull Sound are credited to EU Horizon 2020 project EnFAIT.

The Nova Innovation EnFAIT tidal turbine array is in Bluemull Sound, located in Shetland, Scotland between the islands of Yell and Unst. The tidal array is located just off the Cullivoe headland (Fig. 9). The characterization of the tidal resource present at the site in Bluemull Sound involved the deployment of 3 seabed mounted Nortek Signature 500 ADCPs. The 5 beam ADCPs were deployed in 3 locations north of the three operational M100 turbines at depths of approximately 30-35m, as shown in Fig. 10.

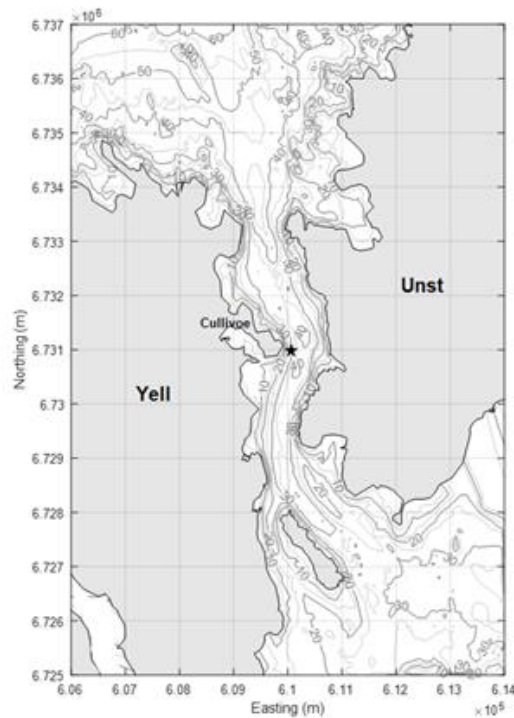


Fig 9. Bluemull Sound

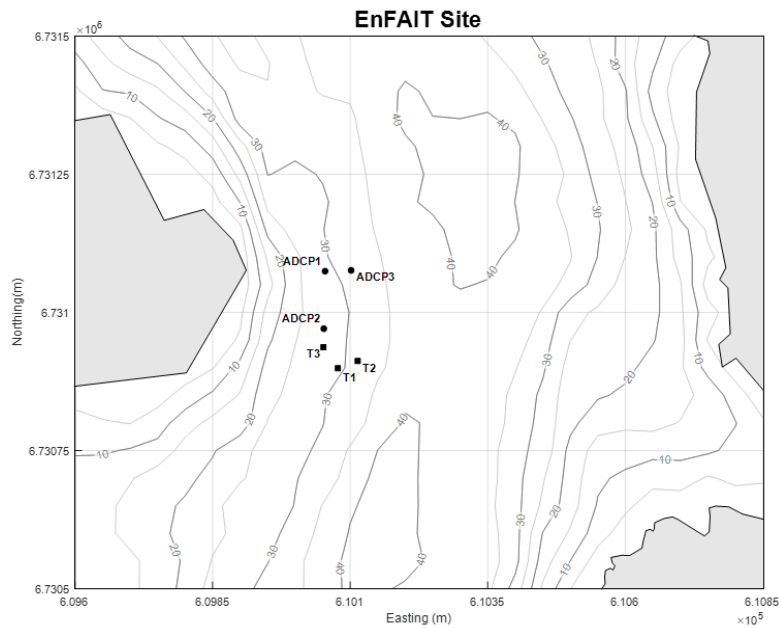


Figure 10. Bluemull Sound site with Turbine (T1, T2 and T3) and ADCP (ADCP1,2, and 3) locations shown.

Considering a blanking distance of 0.5m and mounting point height of ~0.5m, the recorded profiles ranged from ~1m above the seabed to the water surface. The configurations of the ADCP deployments are shown in Table 1. The durations of the deployments of nearly two months captured three full spring to neap tidal cycles for each instrument, with the third also recording surface wave conditions.

Hydrodynamic models were built using Mike 21 software to provide estimated wave and tidal flow conditions across the Bluemull site over a period of 20 years, from 1998 to 2017. Regional bathymetry data from EMODnet, supplemented with high resolution data gathered from a site survey were used to represent the local bathymetry. The Global Self-consistent, Hierarchical, High-resolution Geography (GSHHG) database was utilized to discretize the regional coastline and regional gridded modelled atmospheric data at hourly intervals drove the atmospheric inputs

Table 1 ADCP deployment details

Item	Configuration	Wave Recording
ADCP 1	10 min ave current, concurrent with 850 current samples at 1Hz, starting every 30 mins	No
ADCP 2	Same as ADCP 1	No
ADCP 3	10 min ave current, concurrent with bursts of 800 current and wave tracking samples at 1Hz, starting every 30 mins	Yes

Results

Fig. 11 shows time series of the Sea Surface Height (SSH) and the depth-averaged streamwise velocity. SSH evolves from 31.6m to 34.1 m with a mean of 32.9 m. Tidal variations of SSH and currents are predominantly semi-diurnal and globally symmetric. Peak flood and ebb tidal velocities lag high and low water, respectively, with slack water within 2 hours of the peak flood and ebb tidal velocities occurring.

Histograms of velocity magnitude show that velocity values of 0.5 m/s are exceeded around 90% of time at Bluemull Sound.



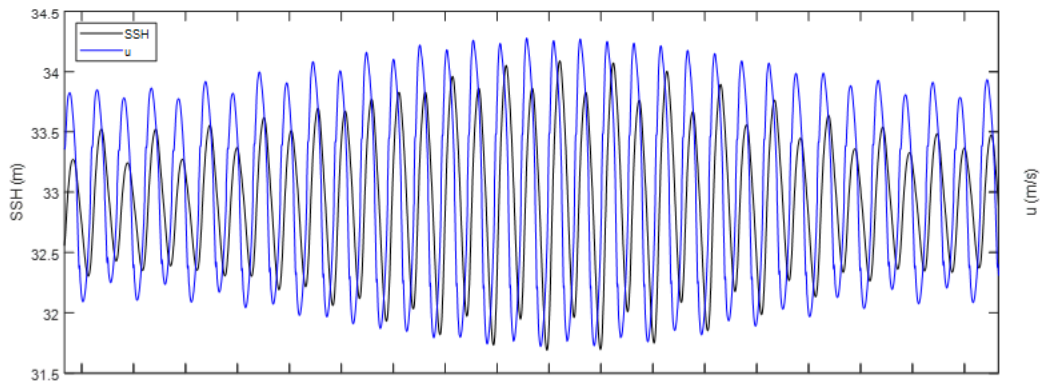


Fig 11. Time series of the sea surface height (SSH) and the depth-averaged streamwise velocity (u) at Bluemull Sound.

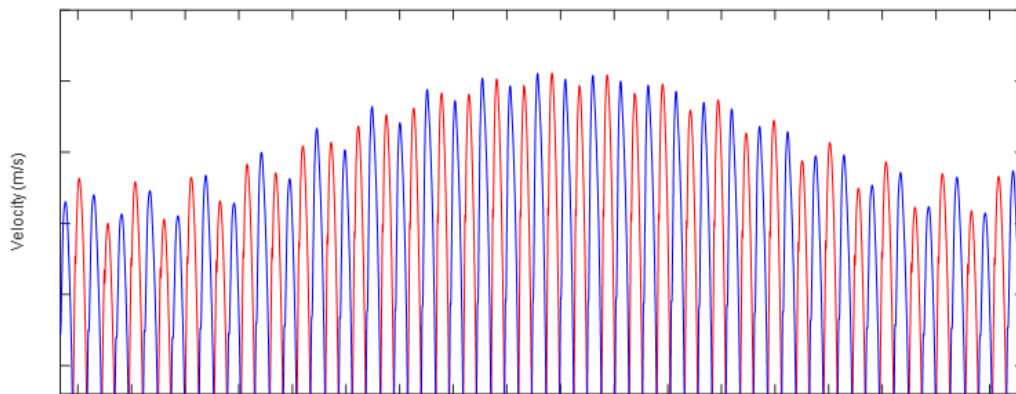


Fig 12. Time series of the depth-averaged velocity magnitude at Bluemull Sound. Red and blue colours are used to identify flood and ebb tide respectively.

While there are differences in the flow from flood to ebb, there is generally good symmetry on flow speed with tidal direction (Fig. 13).

Shown in, Fig. 14, are the recorded site flow velocity shear profiles. For comparison, a power law profile has been included. The ebb profile shows continued flow speed increase towards the surface. This is in line with a typical power law governed profile. The flood profile, however, reaches peak flow speed around the middle of the water column and this is maintained up to the surface. This asymmetry in current speed profile is due to the difference in route to site the flow takes in ebb and flood.

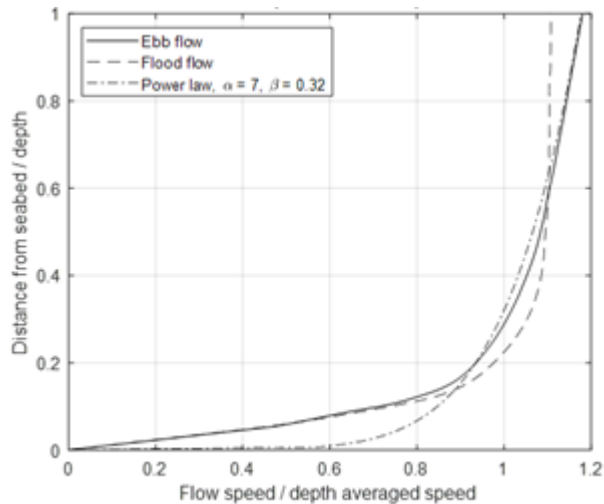


Fig 13. Site flow shear profiles for ebb, flood at Bluemull Sound, and a 7th power law shown for comparison.

In flood the flow is coming out of shallow water to the south and has longer to flow in the channel. These factors mean bottom friction is acting on the flow for longer allowing for the shear profile to develop. In ebb the flow is coming out of deep water to the north, as a result, the shear profile does not have time to fully form.

Turbulence has been characterised by turbulence intensity. Velocity fluctuations have also been taken over 10 minutes intervals. Signal noise is removed to improve the estimate of turbulence intensity.

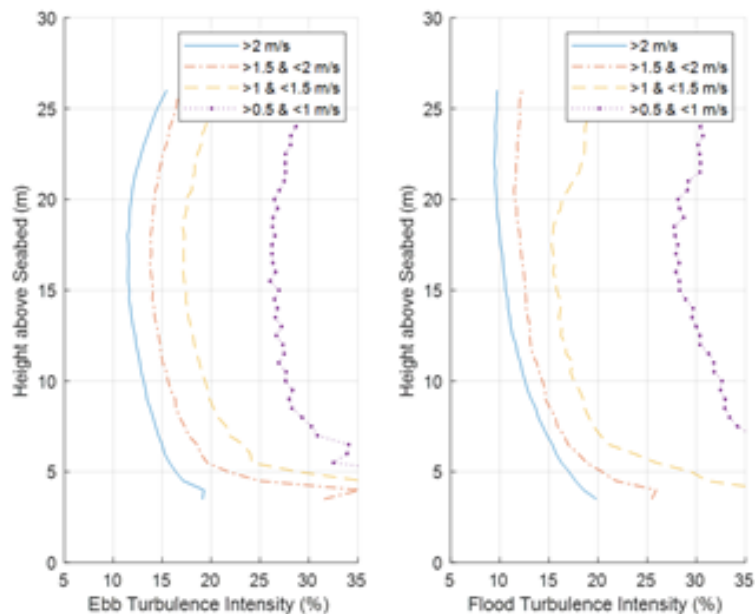


Fig 14. Mean vertical profiles of the turbulence intensity estimated along the streamwise direction.

Turbulence intensity has been found through the water column, for ebb and flood flow, at a range of hub height flow speeds (Fig. 15). Note that there is an increase in turbulence intensity with decreasing flow speed. As turbulence intensity is calculated with velocity as the denominator, a similar level of velocity fluctuation will have a larger turbulence intensity at a lower flow speed. From the analysis performed, in operational flow speeds (generally considered to be $> 1\text{m/s}$) turbulence intensity varies from around 12 to 20%.

Environmental impact monitoring: pre-design work

The design work under the ACAS (Automated Collision Avoidance System) is being conducted by Nova. Within this framework, Nova is undertaking a feasibility assessment of technology options (three main options, see table 1) to monitor near-field interactions between marine life and an operational tidal turbine. FEM has shared its knowledge of marine mammals, birds and fish monitoring experience to inform the selection of sensors and to develop a monitoring strategy for gathering information on interactions between these species groups and operational turbines.

Table 2. Pros and cons of automatic/semi-automatic sensors for monitoring marine mammals, seabirds and fish around a tidal turbine.

	Pros	Cons
Digital cameras	<ul style="list-style-type: none"> • Relatively simple approach • Enables species identification • Can be attached to turbines, reducing complexity of deployment, maintenance and powering. 	<ul style="list-style-type: none"> • Regular maintenance needed (camaras lens been quickly fouled by epibenthic marine organisms) • No data acquisition during hours of darkness, or during conditions of high turbidity • Video processing and analyses are time consuming • Storage requirements of data are considerable
Active sonar devices	<ul style="list-style-type: none"> • Enables data acquisition during conditions of darkness or high turbidity • Real-time processing • Enables data acquisition for non-vocalizing species 	<ul style="list-style-type: none"> • No calibration for species identification (user needs to conduct the calibration) • More expensive than cameras • Poor detection of fish (which swim more rapidly than birds and mammals) • Generally need to be fixed to a structure at a location away from the turbine if seabed mounted, or deployed from a surface vessel. • Air cavitation around turbine blades can affect the resolution and accuracy of results, particularly for smaller targets.
Passive acoustic devices (hydrophones)	<ul style="list-style-type: none"> • Low-cost method • Enable detection and identification of vocalizing species • 3D target localization is possible using arrays of devices • Enables data acquisition during conditions of darkness or high turbidity (for vocalizing species) • Can be attached to turbines and substructures reducing complexity of deployment. 	<ul style="list-style-type: none"> • Non-exhaustive identification of species around the device • Complex data processing and data interpretation. • Storage capacity of devices can quickly be filled by ambient noise in high tidal energy sites.

Acoustics data acquisition has also been discussed, and monitoring marine systems using hydrophones have two main interests: the natural acoustic environment is monitored when the turbine is off, the sound emitted by the turbine can be measured when the turbine is on, and vocalizing animals can be detected and identified within the monitored area. The audiograms are available for some species of mammals, seabirds and fish. Species specific audiograms enable the evaluation of potential acoustic impacts on these animals. A suggestion is to consider one



species that is sensitive to noise emissions to ensure a conservative approach of the definition of environmental impacts of the tidal turbine and subsequent measures to reduce this potential impact.

Also, FEM underlined that depending on the deployment site, the species group on which environmental monitoring is focussed will vary according to regional regulatory regimes and species protection measures. For example, in Canada fish monitoring is a priority while in Shetland, monitoring requirements focus on marine mammals and birds. In the case of fish detection, the combination of optical cameras and acoustic devices might be more useful than the use of sonar systems and cameras.

Following Nova and FEM discussion, the optimal monitoring solution would be to combine digital cameras with sonar (this combination enables the calibration of the sonar system) and applying a medium term monitoring strategy to one or two devices that functions normally (Figure 2). More precisely, and considering only one device, there is a need to:

- set the sonar far enough from the device to take the most advantage of the sonar coverage angle of 120°;
- set up three digital cameras in order to get images of marine life that moves in 3D around the device;
- enable monitoring during normal turbine operations in order to gather information on the behavior of animals around operational devices.

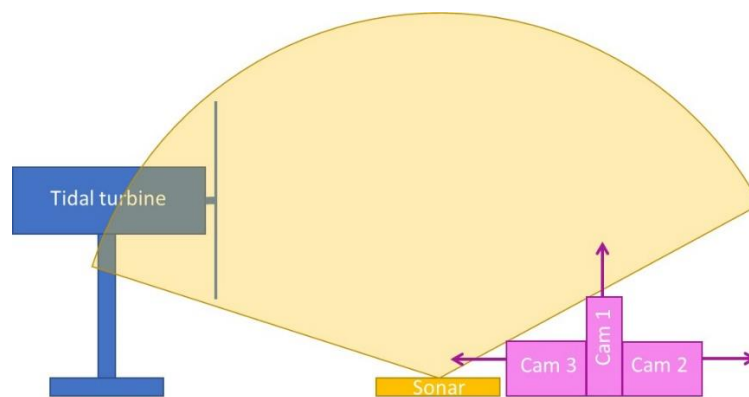


Fig 15. Schematic view of the monitoring design of one tidal turbine in order to gain data on the marine species using the area around the turbine (nota: not at scale)

Duration of deployment would ideally account for any inter-annual variability in addition to intra-annual variability. Multiple years of deployment would also enable sufficient data to be gathered for meaningful analysis and refinement of encounter modelling parameters, since monitoring at Bluemull Sound and other tidal sites has indicated that wildlife interactions with turbines are likely to be rare events.

This monitoring strategy would enable data to be gathered to enable a better assessment of the risk of near-field encounters between birds/mammals/fish and tidal turbines. This in turn will enable the refinement of encounter and collision risk models using more exhaustive and realistic data. The data gained following this monitoring design would particularly help at more thoroughly defining proportions of marine fauna that move through the sonar detection angle and building species-specific behavioral responses to operational turbines (e.g. no response, evasive response, etc.).

Several key considerations (e.g. sensors orientation) need however to be considered in order to ensure the success of data acquisition. A recent review of the monitoring technologies and technics for detecting interactions between marine animals and turbines have been published (Hasselman D. et al., 2020) and provides tracks to enhance monitoring design around tidal energy devices.

Perspectives

A new characterization campaign will start in summer 2020 at Etel River test site. The next report will present the Reynolds stresses which will result from the upcoming five-beam ADCP measurements. The Doppler noise identified in the present dataset does not allow to properly quantify these turbulence metrics. The site characterization on a more ecological point of view will also be presented in the next report with the results of the biocolonisation survey (temporal and small spatial scale variability) and the influence of environmental variables (turbulence and current, temperature, salinity, nutrients, dissolved oxygen, pH, turbidity), which will be measured simultaneously, will be analyzed. The next report will also include information on the refinement of the collision risk model designed by NOVA and the subsequent improvements of the environment impact module of the DTOceanPlus model. The environmental impacts of the tidal turbine will be calculated before and after DTOceanPlus improvements.



References

Hasselman, D.J., D.R. Barclay, R.J. Cavagnaro, C. Chandler, E. Cotter, D.M. Gillespie, G.D. Hastie, J.K. Horne, J. Joslin, C. Long, L.P. McGarry, R.P. Mueller, C.E. Sparling, and B.J. Williamson. 2020. Environmental Monitoring Technologies and Techniques for Detecting Interactions of Marine Animals with Turbines. In A.E. Copping and L.G. Hemery (Eds.), OES-Environmental 2020 State of the Science Report: Environmental Effects of Marine Renewable Energy Development Around the World. Report for Ocean Energy Systems (OES). (pp. 176-213).

I. A. Milne, R. N. Sharma, R. G. J. Flay, and S. Bickerton, "The role of onset turbulence on tidal turbine blade loads," in Proc. 17th Australasian Fluid Mechanics Conference, Auckland, NZ, 2010.

A. Sentchev, M. Thiébaud, and F. G. Schmitt, "Impact of turbulence on power production by a free-stream tidal turbine in real sea conditions," *Renewable Energy*, vol. 147, pp. 1932–1940, 2019.

M. Thiébaud, J.-F. Filipot, C. Maisondieu, G. Damblans, R. Duarte, E. Droniou, N. Chaplain, and S. Guillou, "A comprehensive assessment of turbulence at a tidal-stream energy site influenced by wind-generated ocean waves," *Energy*, vol. 191, p. 116550, 2020.

M. Guerra and J. Thomson, "Turbulence Measurements from Five-Beam Acoustic Doppler Current Profilers," *Journal of Atmospheric and Oceanic Technology*, vol. 34, no. 6, pp. 1267–1284, 2017.

